XIV International Conference on Computational Plasticity. Fundamentals and Applications
COMPLAS 2019
E. Oñate, D.R.J. Owen, D. Peric , M. Chiumenti, and Eduardo de Souza Neto (Eds)

FORMULATION METHOD OF BALL INDENTATION PROCESS FOR ULTRA-THIN ELASTIC BODY WITH MECHANICS POISSON EFFECT

CHAO LU [*] AND ATSUSHI SAKUMA [†]

[*] Graduate School of Science and Technology
Kyoto Institute of Technology
Matsugasaki, Sakyo-ku, 606-8585 Kyoto, Japan
e-mail: michaellu950609@gmail.com, http://www.fibro.kit.ac.jp/

[†] Division of Textile Science
Kyoto Institute of Technology
Matsugasaki, Sakyo-ku, 606-8585 Kyoto, Japan
email: sakuma@kit.ac.jp, http://www.fibro.kit.ac.jp/

Key words: Finite Element Method, Full Contact Model, Poisson's Effect, Engineering Strain

Abstract. *A new theoretical method for determining the mechanics properties of ultra-thin elastic materials is proposed in this paper. This method is based on a full contact model and Poisson's effect. This study consisted of three steps. First, FE model of indentation problem for ultra-thin specimen is developed by elastic constitutive relationship for precise analysis of problem. Second, the simplified model is used to evaluate the result of FEM, and its availability is discussed by comparison with extended Hertzian theory. Third, an equation is proposed after comparing the results of FEM, extended Hertzian theory and full contact model.*

1 INTRODUCTION

Over the past one hundred years, the indentation technique has been adopted to measure the hardness and elastic modulus of various materials [1-3]. Fundamental ball indentation technology proposed by Heinrich Hertz is regarded as an effective method for deducing the physical properties of semi-infinite elastic bodies [1]. W.C Oliver *et al* proposed a nanoindentation technique applied under small-scale deformation [4]. After that, experiments on nanoindentation were carried out continuously [5-7]. Several researchers have theoretically investigated the mechanical properties for thin film materials. However, the studies of Hertzian theory and nanoindentation technique have limitation when one of the contacting bodies is very thin. A extended Hertzian theory based on nonequivalent indentation strain was proposed by Tani *et al*. to investigate the applicability in this case [8,9]. but this method is not universal and has a certain error when the thickness is too small.

In this paper, therefore, a theoretical full contact theory is studied to solve this theoretically problem. First, the optimal experimental conditions were selected after considering the thickness effect and diameter effect. Then, a simplified model is formulated to derive full contact theory. At last, by using the result of FEM, the difference between extended theory and full contact theory is compared under various thickness conditions.

2. EVALUATION METHOTOLOGY

2.1 Thickness effect by FEM

The FE model of indentation problem is developed by elastic constitutive relationship for precise analysis. The intent of this section is to explore the effects of various dimensions of the diameter and specimen on the experiment and to find optimal experimental conditions. Numerical experiments have been carried out by LS-DYNA and FEMAP V11.4.1.

The boundary conditions for FE model of ultra-thin indentation problem are given in Fig.1.

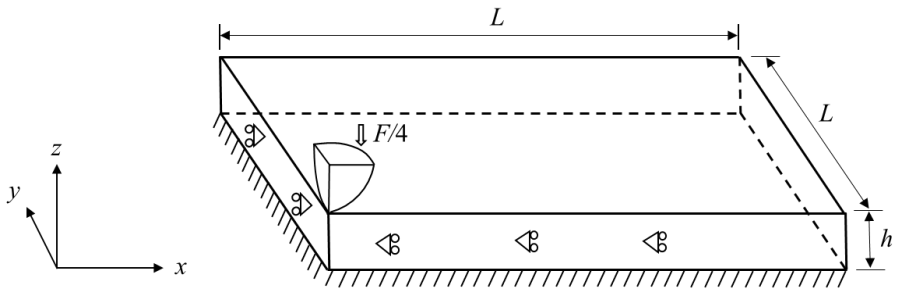

Figure 1: Geometry and boundary conditions of quarter finite element model

The FE models of indenter and specimen were constructed and meshed in FEMAP. The FE models and its meshing at different thickness *h* of specimen are given in Fig.2. The diameter of indenter is 30mm. Since the symmetricity of this model, a quarter of specimen and a spherical shell of indenter are used to reduce computation time. Specimen is a rectangular parallelepiped with a side length of 50mm×50mm. Its thickness *h* is prepared as 50mm, 10mm and 1mm for corresponding to different situations. The regional differential meshing is used for specimen. In particular, the model can be neglect its dimensions as shown in Fig.2 (c) when the thickness of the specimen is very thin.

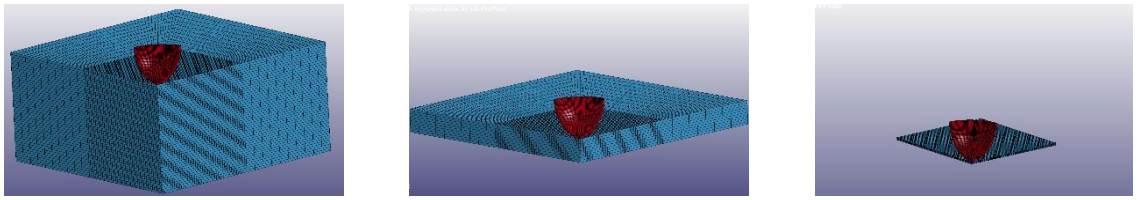

(a) Thick (Hertzian) (b) Thin (extended) (c) Ultra-thin (full contact)

Figure 2: FE models to analyze the influence of thickness

Fig.3 shows the thickness effect on the experimental results. It indicates that the same indentation depth produces different magnitudes of load force *F* at different thicknesses. On the other hand, this difference becomes more and more noticeable when the thickness becomes thinner.

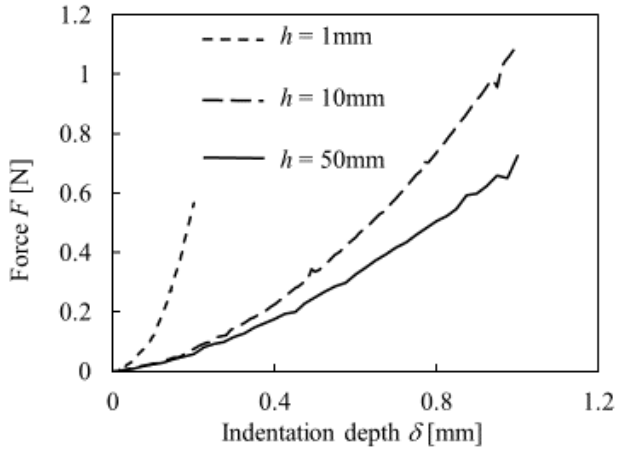

Figure 3: Thickness effect in indentation

2.2 Diameter effect for ultra-thin specimen

The diameter effect is discussed in this section. The FE models are shown in Fig.4. The indenter is a rigid sphere with a diameter of 2mm and 30 mm. Where only a portion of a spherical indenter is taken for the indenter model in order to reduce the simulation time.

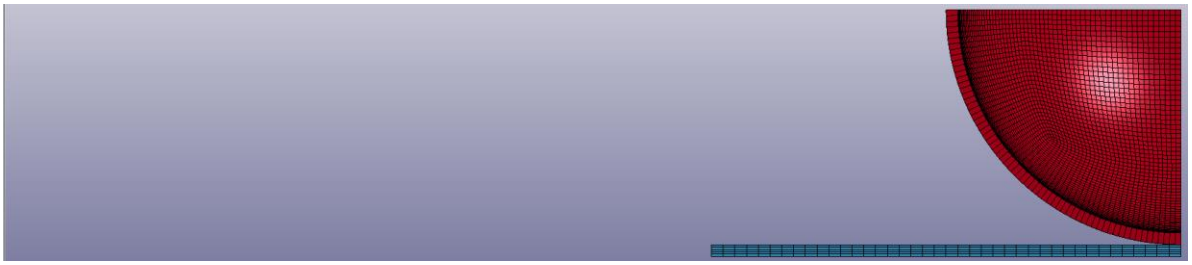

(a) Diameter ϕ=2mm

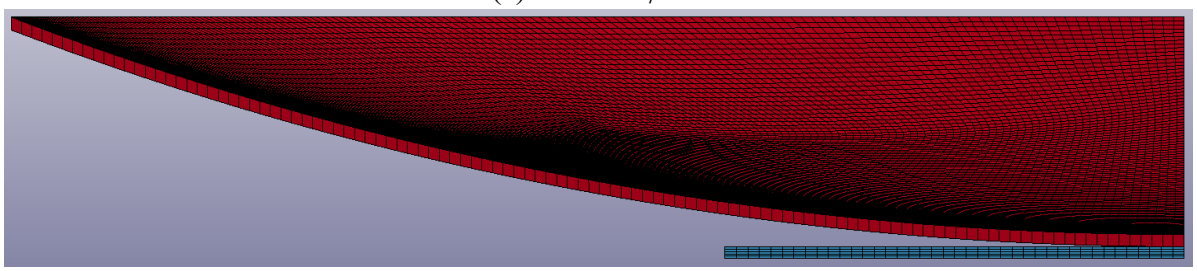

(b) Diameter ϕ=30mm

Figure 4: Finite element mesh of ultra-thin indentation problem at different diameter of indenter

Table 1 represents the conditions of experiment. The Young's modulus E and Poisson's ratio v of indenter are 200GPa and 0.29, respectively. The Young's modulus E of specimen is 100kPa, and the Poisson ratio v is 0.45.

Table 1: Experiment condition

	Unit	Indenter	Specimen
Materials		rigid	elastic
Young's modulus	E [Pa]	200G	100k
Poisson's ratio		0.29	0.45
Diameter/ Thickness	ϕ/h [mm]	2, 30	0.05

Fig.5 shows the diameter effect of thin specimen indentation test. It indicates that the larger diameter h of indenter will cause the bigger load force F under the same experimental conditions. The large diameter indenter is used in this study in order to facilitate the processing and comparison of experiment results.

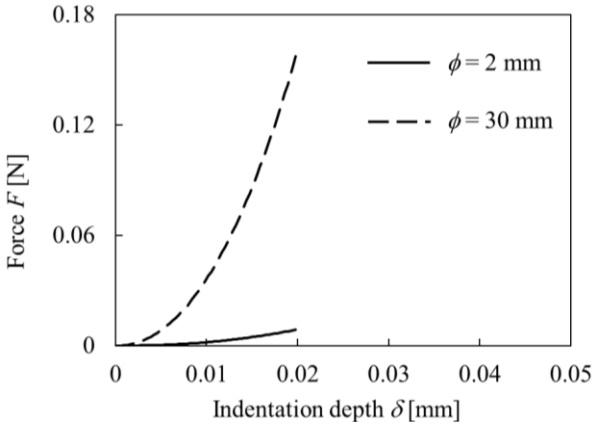

Figure 5: Diameter effect in thin specimen

3. EVALUATION FOR ULTRA-THIN INDENTATION PROBLEM

3.1 Evaluation by extended Hertzian theory

The relationship between the load force F and the indentation depth δ shown in the Fig.1 (a) can be described by Hertzian contact theory [1] as following.

$$F = \frac{4}{3}\frac{E}{1-v^2}\left(\frac{\phi}{2}\right)^{\frac{1}{2}}\delta^{\frac{3}{2}} = A\delta^{\frac{3}{2}} \tag{1}$$

$$A = \frac{4}{3}\frac{E}{1-v^2}\left(\frac{\phi}{2}\right)^{\frac{1}{2}} \tag{2}$$

Here ϕ, E and v are the diameter of indenter, the Young's modulus and Poisson's ratio of specimen, respectively. Equation (3) is the extended Hertzian theory proposed by Tani *et al.* [8,9] as shown in Fig.1 (b). Where coefficient B is the constant determined by the curve fitting method numerically.

$$\hat{F} = A\{\delta(1+B\delta)\}^{\frac{3}{2}} = \hat{A}\delta^{\frac{3}{2}} \tag{3}$$

$$\hat{A} = A(1+B\delta)^{\frac{3}{2}} \tag{4}$$

Therefore, the apparent Young's modulus $\hat{E}$ of the specimen during the experiment can be determined by Equation (5).

$$\hat{E} = E(1 + B\delta)^{\frac{3}{2}} \tag{5}$$

3.2 Formulation of full contact theory

The relationship between load force F and indentation depth δ represents an important material characteristic. However, it is very difficult to analyses the contact mechanics when one of the contacting bodies is very thin. The aim of this section is to seek a theoretical method to express the load force F according to indentation depth δ when thickness h is very thin.

Fig.6 shows a schematic of model named full contact model for the ultra-thin indentation problem. It differs from the Hertzian contact theory in the contact area radius a, which is denoted by α in this paper. The shaded portion in Fig.6 is considered to be the compressed area. A coordinate system is established with the projection point of the indenter on the bottom surface as the origin. Where δ is the indentation depth, h is the thickness of specimen, δ_i and h_i are the indentation depth and thickness of specimen at radius r_i on the r-axis, respectively. α is the radius of the contact area which can be determined by equation (6).

$$\alpha = \sqrt{\phi\delta - \delta^2} \tag{6}$$

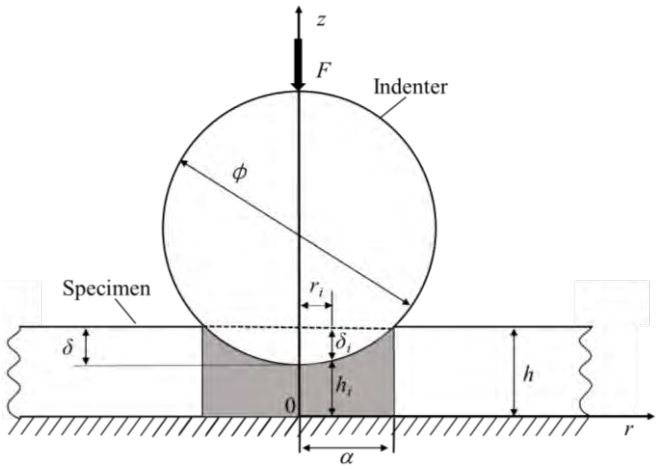

Figure 6: Schematic of full contact theory model

The curve equation of the indenter can be expressed by the equation (7).

$$z = h + \frac{\phi}{2} - \delta - \sqrt{\frac{\phi^2}{4} - r^2} \tag{7}$$

$$r \in [0, \alpha]$$

When the value of r increase from 0 to α, the expressions of δ_i and h_i are as shown in equation (8) and equation (9).

$$\delta_i = \delta - \frac{\phi}{2} + \sqrt{\frac{\phi^2}{4} - r_i^2} \tag{8}$$

$$h_i = h + \frac{\phi}{2} - \delta - \sqrt{\frac{\phi^2}{4} - r_i^2} \tag{9}$$

According to the definition of engineering strain, the strain is the ratio of the shortening or elongation of the specimen to the initial value of the gauge length. Therefore, the strain ε_i at different positions can be defined by equation (10).

$$\varepsilon_i = \frac{\delta - \frac{\phi}{2} + \sqrt{\frac{\phi^2}{4} - r_i^2}}{h} \tag{10}$$

The stress value σ_i at different positions r_i can be obtained by Hooke's law $\sigma = E\varepsilon$, where E is the Young's modulus of the specimen.

$$\sigma_i = E\frac{\delta - \frac{\phi}{2} + \sqrt{\frac{\phi^2}{4} - r_i^2}}{h} \tag{11}$$

In order to simplify the model, the Young's modulus of the specimen is considered as a constant. Therefore, the load force F can be defined by equation (12).

$$F = \int_0^{\alpha} 2\pi\sigma(r)dr = 2\pi E\int_0^{\alpha} r\frac{\delta - \frac{\phi}{2} + \sqrt{\frac{\phi^2}{4} - r_i^2}}{h}dr \tag{12}$$

When the sides of the object is fixed, the boundary creates an extra force on the object during compression process. This effect is called the Poisson effect which can be defined as shown in equation (13). Where v is the Poisson's ratio of specimen.

$$E' = E\frac{1 - v}{(1 + v)(1 - 2v)} \tag{13}$$

In the ultra-thin ball indentation test, the compressed area can be approximated as the shaded portion in Fig. 6. Therefore, the full contact theory is proposed as shown in equation (14).

$$F = \frac{\pi E\delta^2}{h}\left(\frac{\phi}{2} - \frac{\delta}{3}\right)\frac{1 - v}{(1 + v)(1 - 2v)} \tag{14}$$

3.3 Evaluation and comparison

Based on the full contact theory, the fundamental and extended Hertzian theories, a series of experiments were conducted to investigate the differences in various thicknesses h of specimen.

The FE model used in this section is similar to that of Fig.4, and the mechanical properties of the material are the same as in Table.1. The diameter of the indenter is set to 30mm because of the diameter effect, while the thickness h of the specimen is 0.05mm, 0.1mm, 0.3mm, 1mm and 3mm. The direction of indenter is perpendicular to the specimen bottom surface. Since the thickness h of each specimen is different, the maximum indentation depth is set to 20% of the specific thickness h of specimen in order to visually compare the differences.

The calculated results are shown in Fig.7. It indicated when the thickness of the specimen is decreasing, the results obtained by the full contact theory are getting closer to the FEM results. The results are almost the same when the thickness reaches 0.1mm or even 0.05mm. On the other hand, the extended Hertzian theory is very close to the FEM results at different thickness h of specimen.

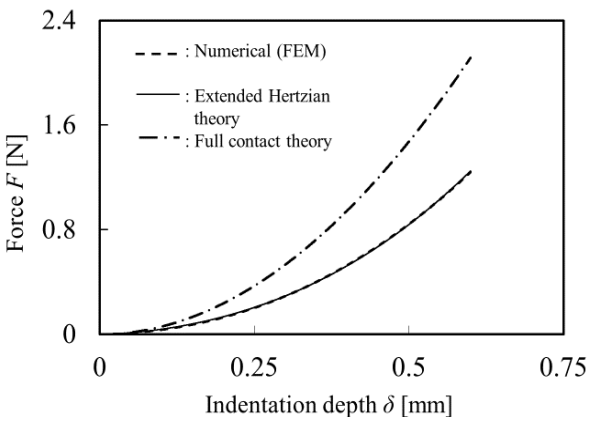

(a) Thickness h=3mm

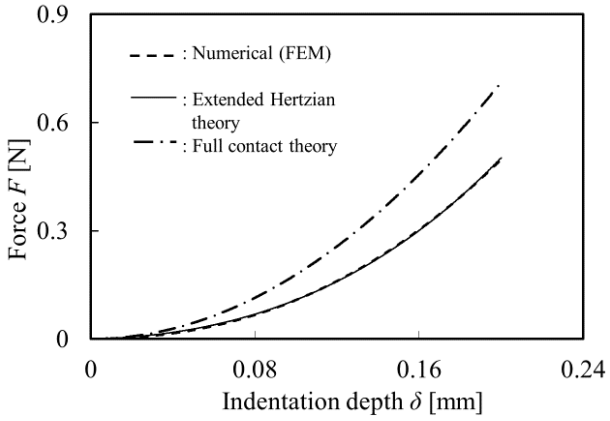

(b) Thickness h=1mm

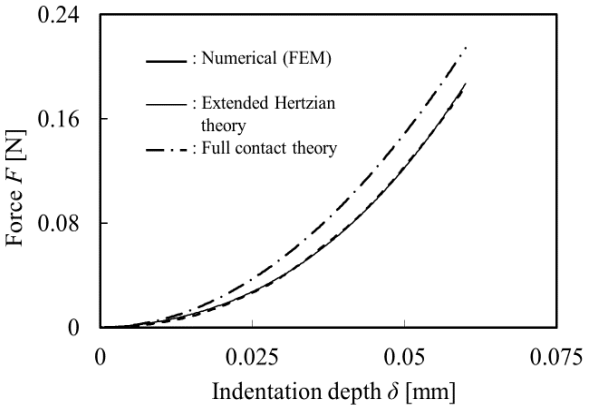

(c) Thickness h=0.3mm

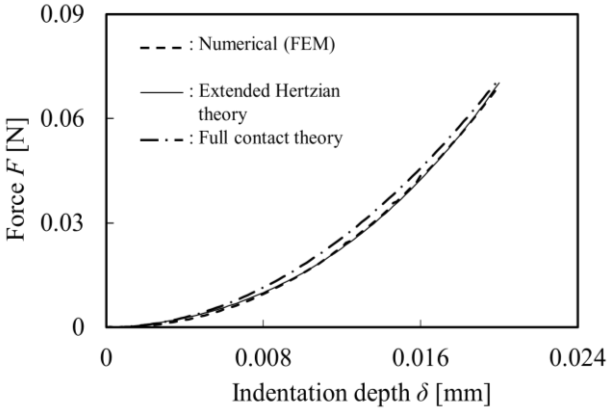

(d) Thickness h=0.1mm

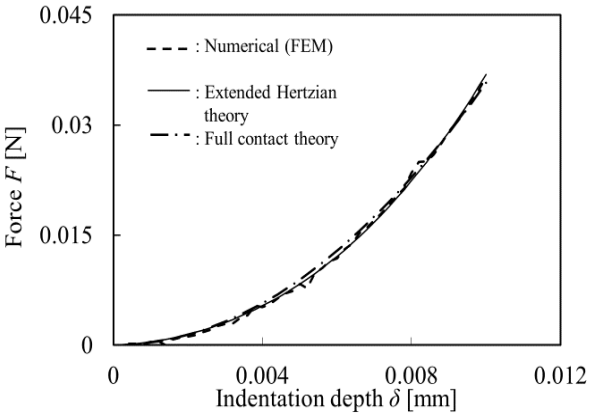

(e) Thickness h=0.05mm

Figure 7: Comparison of different theories

Fig. 8 shows the variation of E'/E_0 at different thicknesses. Where E_0 is the actual Young's modulus which the value is 100kPa. F' is the load force obtained from FE results. E' is the apparent Young's modulus obtained in the simulation according to the full contact theory. The solution of E' is as shown in equation (15). The abscissa is the thickness h, and the ordinate is the ratio of the apparent Young's modulus E' to the actual Young's modulus E_0. It indicates that the apparent Young's modulus E' decreases as the thickness of the specimen increases.

$$E' = \frac{F'}{C} \tag{15}$$

$$C = \frac{\pi\delta^2}{h}\left(\frac{\phi}{2} - \frac{\delta}{3}\right)\frac{1-\upsilon}{(1+\upsilon)(1-2\upsilon)}$$

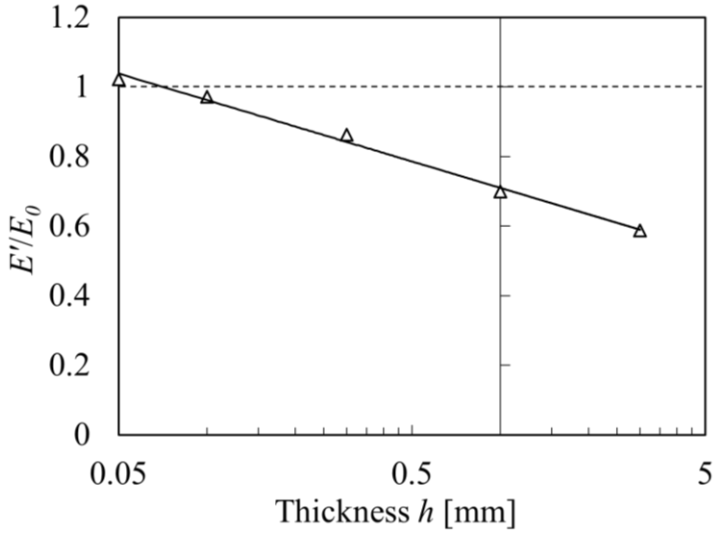

Figure 8: Variation of Young's modulus E' at different thicknesses

The results can be fitted with a logarithmic function as shown in equation (16). The coefficient of determination R^2 is 0.9931.

$$\frac{E'}{E_o} = -0.11\ln(h) + 0.7098 \tag{16}$$

It can be obtained that when h is 0.0715 mm, apparent Young's modulus E' is equal to actual Young's modulus E_0. Therefore, it can be considered that full contact theory is applied when the thickness is less than 0.0715 mm.

$$R_L = \frac{h}{\phi} \tag{17}$$

Here， R_L is the ratio of thickness h to diameter ϕ. In this paper, the full contact theory can be applied when the value range of R_L is 0.0017 which is threshold of applicability of equation (14).

4 CONCLUSION

- The results of the experiment indicate that the extended Hertzian theory has good applicability, and the full contact theory applies only when the thickness h of specimen is very thin.
- By comparing the extended Hertzian theory with the full contact theory, it can be found that the full contact theory can predict the result directly when h is very thin.
- According to the principle of geometric similarity, the full contact theory can be applied when the ratio R_L of the thickness h to the diameter ϕ is under 0.0017 in the case of very thin specimen.

REFERENCES

[1] Hertz, H. R. *Über die Berührung fester elastischer Körper und über die Härte*. Universitätsbibliothek Johann Christian Senckenberg, (2006).

[2] Oliver, W. C., and George M. P. An improved technique for determining hardness and elastic modulus using load and displacement sensing indentation experiments. *Journal of materials research* (1992) **7.6**: 1564-1583.

[3] Oliver, W. C., and George M. P. Measurement of hardness and elastic modulus by instrumented indentation: Advances in understanding and refinements to methodology. *Journal of materials research* (2004) **19.1**: 3-20.

[4] Pharr, G. M., and W. C. Oliver. Measurement of thin film mechanical properties using nanoindentation. *Mrs Bulletin* (1992) **17.7**: 28-33.

[5] Nayebi A, El Abdi R, Bartier O, et al. New procedure to determine steel mechanical parameters from the spherical indentation technique. *Mechanics of Materials*, (2002) **34(4)**: 243-254.

[6] Ma D, Xu K, He J. Numerical simulation for determining the mechanical properties of thin metal films using depth-sensing indentation technique. *Thin Solid Films*, (1998) **323(1-2)**: 183-187.

[7] Waters, N. E. The indentation of thin rubber sheets by spherical indentors. *British Journal of Applied Physics* (1965) **16.4**: 557.

[8] Tani, M., Sakuma, A., and Shinomiya, M. Evaluation of thickness and Young's modulus of soft materials by using spherical indentation testing. *Transactions of the Japan Society of Mechanical Engineers, Series A* (2009) **75.755**: 901-908.

[9] Tani, M., and Sakuma, A. Applicability evaluation of Young's modulus measurement using nonequivalent indentation strain in spherical indentation testing for soft materials. *Transactions of the Japan Society of Mechanical Engineers, Series A* (2010) **76.761**: 102-108.